ARTICLE
Journal of Cellular Biochemistry 105:391–403 (2008)

Journal of Cellular Biochemistry

Identifying Functional Neighborhoods Within the Cell Nucleus: Proximity Analysis of Early S-Phase Replicating Chromatin Domains to Sites of Transcription, RNA Polymerase II, HP1γ, Matrin 3 and SAF-A

Kishore S. Malyavantham,[1] Sambit Bhattacharya,[2] Marcos Barbeitos,[1] Lopamudra Mukherjee,[3] Jinhui Xu,[3] Frank O. Fackelmayer,[4] and Ronald Berezney[1*]

[1]*Department of Biological Sciences, University at Buffalo, Buffalo, New York 14260*
[2]*Department of Mathematics & Computer Sciences, Fayetteville State University, Fayetteville, North Carolina 28311*
[3]*Department of Computer Sciences and Engineering, University at Buffalo, Buffalo, New York 14260*
[4]*Biomedical Research Institute, Foundation for Research & Technology, Hellas, 45110 Ioannina, Greece*

ABSTRACT

Higher order chromatin organization in concert with epigenetic regulation is a key process that determines gene expression at the global level. The organization of dynamic chromatin domains and their associated protein factors is intertwined with nuclear function to create higher levels of functional zones within the cell nucleus. As a step towards elucidating the organization and dynamics of these functional zones, we have investigated the spatial proximities among a constellation of functionally related sites that are found within euchromatic regions of the cell nucleus including: HP1γ, nascent transcript sites (TS), active DNA replicating sites in early S-phase (PCNA) and RNA polymerase II sites. We report close associations among these different sites with proximity values specific for each combination. Analysis of matrin 3 and SAF-A sites demonstrates that these nuclear matrix proteins are highly proximal with the functionally related sites as well as to each other and display closely aligned and overlapping regions following application of the minimal spanning tree (MST) algorithm to visualize higher order network-like patterns. Our findings suggest that multiple factors within the nuclear microenvironment collectively form higher order combinatorial arrays of function. We propose a model for the organization of these *functional neighborhoods* which takes into account the proximity values of the individual sites and their spatial organization within the nuclear architecture. J. Cell. Biochem. 105: 391–403, 2008.

KEY WORDS: RNA POLYMERASE II SITES; HP1γ SITES; REPLICATION SITES; TRANSCRIPTION SITES; CELL NUCLEUS; PROLIFERATING CELL NUCLEAR ANTIGEN; NUCLEAR MATRIX; MATRIN 3; SAF-A; COMPUTER IMAGE SEGMENTATION; PROXIMITY ANALYSIS; PATTERN RECOGNITION IMAGE ANALYSIS; MINIMAL SPANNING TREE NETWORKS

Despite significant advances in molecular biology and biochemistry, our understanding of the nucleus is at its infancy. The genome is more than a linear sequence of DNA [Misteli, 2007] and is segmented into chromosomes which occupy distinct territories in the interphase cell nucleus [Cremer et al., 2001]. Chromatin within these chromosomes is arranged into multiple levels of hierarchical organization from the nucleosomal 10 nm arrays to the 30 nm fibers to chromatin loops and higher order domains [Berezney, 2002; Cremer et al., 2006; Razin et al., 2007]. Although the eukaryotic nucleus is devoid of any internal membranes, it introduces an incredible level of complexity and several layers of control, which regulate the genomic functions and increase the efficiency of processivity and enzyme regulatory mechanisms. Moreover, the compartmentalization of genomic functions and factors that mediate these functions suggests a high level of structural organization [Berezney et al., 1996; Strouboulis

Abbreviations used: DAPI, 4′,6-diamidino-2-phenylindole; HP1γ, heterochromatin protein 1, gamma; MST, minimal spanning tree; PCNA, proliferating cell nuclear antigen; Pol II, RNA polymerase II sites; RS, replication sites; SAF-A, scaffold attachment factor–A; TS, transcription sites.

Grant sponsor: National Institutes of Health; Grant number: GM 072131; Grant sponsor: National Science Foundation; Grant number: IIS-0713489.

*Correspondence to: Ronald Berezney, Department of Biological Sciences, University at Buffalo, Buffalo, NY 14260. E-mail: berezney@buffalo.edu

Received 11 May 2008; Accepted 13 May 2008 • DOI 10.1002/jcb.21834 • 2008 Wiley-Liss, Inc.
Published online 10 July 2008 in Wiley InterScience (www.interscience.wiley.com).

and Wolffe, 1996; Dundr and Misteli, 2001; Hendzel et al., 2001; Berezney, 2002; Stein et al., 2004, 2003b, 2007; Meaburn and Misteli, 2007].

A striking example which reflects this compartmentalization is the identification of 1 megabase pair (Mbp) chromatin domains that replicate in early S-phase [Jackson and Pombo, 1998; Ma et al., 1998] and are enriched in actively transcribed genes [MacAlpine et al., 2004; Schubeler et al., 2004]. These chromatin domains persist throughout the cell cycle in a dynamic state and are capable of participating in a variety of genomic functions [Ma et al., 1998; Sadoni et al., 2004; Albiez et al., 2006]. Other studies have defined transcription sites in the cell nucleus [Jackson et al., 1993; Wansink et al., 1993; Iborra et al., 1996; Wei et al., 1999]. In addition, the protein factors which mediate and regulate genomic function, also form punctate domains [Hendzel et al., 2001; Stein et al., 2003a,b; Young et al., 2004; McManus et al., 2006; Mitchell and Fraser, 2008]. Recent studies of these punctate sites indicate their role in the combinatorial organization of several enzymatic and regulatory complexes within the vicinity of the participating chromatin domains [Verschure et al., 2002; Stein et al., 1999, 2004]. These factors further determine the ''nuclear microenvironment'' around the gene foci and the potential activities engaged in by the chromatin domains encompassing these genes [Young et al., 2004; Stein et al., 2005, 2007; Zaidi et al., 2006].

Using 3-D microscopy and computer imaging techniques, Wei et al. [1998] demonstrated that DNA replication and transcription sites in early S-phase are clustered into separate higher order ''zones'' in the nucleus. These separate zones of replication and transcription are in close apposition and form distinct network-like patterns in 3-D [Wei et al., 1998]. The dynamic interplay of these ''functional zones'' was implicated as the structural basis for the intricate coordination of genomic functions in the nucleus [Berezney and Wei, 1998; Cook, 1998; Berezney, 2002]. Moreover, several studies reported the presence of specialized zones for various genomic functions, protein factors and epigenetic modifications of the chromatin [Stein et al., 1999; Zinner et al., 2006; Skalnikova et al., 2007]. While the structural basis for nuclear zoning is not known, Wei et al. (1999) demonstrated that the replication and transcription zones are maintained following extraction of cells for nuclear matrix.

In this investigation we examine the structural organization of early S-replicating chromatin domains in relationship to transcription sites, RNA polymerase II and HP1γ sites, respectively. The proximity relationships of the labeled functional and protein factor sites was determined using a newly developed computer image program. The relationships of these sites to the overall nuclear architecture was then examined using two abundant nuclear matrix proteins, matrin 3 [Belgrader et al., 1991; Nakayasu and Berezney, 1991] and SAF-A/hnRNP-U [Fackelmayer et al., 1994; Kipp et al., 2000] and application of the minimal spanning tree (MST) pattern recognition algorithm to visualize higher order network-like patterns [Dussert et al., 1987, 1988]. Based on our findings, a model of ''nuclear functional neighborhoods'' is proposed in which the functional and protein factor sites are in close spatial proximity to each other and to a network-like nuclear matrix architecture, forming distinct zones of combinatorial associations and activities within the euchromatic compartments.

MATERIALS AND METHODS

CELL CULTURE AND GENERATION OF A HeLa CELL LINE STABLY EXPRESSING PCNA-GFP

All experiments were performed on exponentially growing HeLa cells [ATCC number CCL-2] in Advanced DMEM (Invitrogen, Carlsbad, CA) supplemented with Gluta-Max^{TM}, 1% Penicillin–Streptomycin antibiotic solution (Invitrogen, Carlsbad) and 2.5% fetal bovine serum (Invitrogen, Carlsbad). Cells were grown (37°C and 5% CO_2) on glass cover slips (12CIR-1, Fisher Scientific) 12–15 h before the labeling experiments. A clone of HeLa cells stably expressing PCNA-GFP fusion protein was used in experiments that involve labeling of DNA replication sites in early S-phase. cDNA for the gene PCNA was first released from pUHD (PCNA/GFP) 10–3 vector [Somanathan et al., 2001] by digesting with Sal1 and Age1 restriction enzymes (Promega, Madison, WI). This insert was cloned in frame into the multiple cloning site of pEGFP N-1 (Clontech, Palo Alto, CA) which has sites for Sal1 and Age1. The resulting PCNA-GFP fusion has a five amino acid (QPVAT) linker peptide between C-terminus of PCNA and N-terminus of GFP. HeLa cells were then transfected with this PCNA-GFP-N1 construct using Lipofectamine and Plus reagents according to the manufacturer's recommendation (Invitrogen, La Jolla, CA). Colonies expressing the fusion protein stably were isolated by G418 antibiotic selection (600 μg/ml) for 10 to 14 days. Suitable colonies expressing moderate amounts of PCNA-GFP fusion protein stably were selected by visual observation under the inverted fluorescence microscope, marked and transferred into 12-well plates for further amplification using sterile trypsinized filter paper discs. One such colony (PCNA-GFP-N1-2) was observed to stably express moderate amounts of PCNA-GFP fusion protein and was used for all experiments that involved PCNA-GFP labeling.

VISUALIZATION OF FUNCTIONAL SITES BY INDIRECT IMMUNOFLUORESCENCE

For in vivo labeling of transcription, exponentially growing HeLa cells were pulsed with FU (1 mM) for 10 min. Cells were washed with 1 X PBS and fixed with 4% para-formaldehyde for 10 min. This and all subsequent steps were performed at room temperature. Fixed cells were permeabilized with 0.5% Triton X-100 for 20 min, followed by pre-blocking with 10% FBS for 15 min. Transcription sites are then labeled by sequential incubations with rat anti-BrdU monoclonal antibody (1:50 dilution, Sera-Lab) followed by anti-rat-IgG conjugated to Alexa647 (Molecular Probes). To label for RNA pol II, HP1γ, matrin 3 or SAF-A sites, fixed cells are incubated simultaneously with the respective primary antibodies and subsequently with host specific secondary antibodies conjugated to Alexa488 or Alexa594. Cells were selected for visualization by means of their early S replication patterns [Vogel et al., 1989; Fox et al., 1991; Dimitrova and Berezney, 2002]. The PCNA-GFP signal was enhanced with mouse or rabbit anti-GFP antibodies conjugated to Alexa488 dye (Molecular Probes, Invitrogen Corp.). Primary antibodies used in the immunolabeling experiments were rabbit polyclonal antibodies to HP1γ (ab10480, Abcam, Inc., Cambridge,

MA) and SAF-A/hnRNP-U [Fackelmayer et al., 1994], monoclonal mouse antibodies (IgG) to RNA polymerase II (ARNA-3, RDI division of Fitzgerald industries) and polyclonal chicken antibodies to matrin 3 [Belgrader et al., 1991]. All secondary antibodies were cross-adsorbed for any inter-species reactivity (Molecular Probes, Invitrogen Corp.) and are described in the figure legends. Prolong gold anti-fade reagent was used for mounting (Molecular Probes, Invitrogen Corp.).

IN SITU NUCLEAR MATRIX EXTRACTION

For in situ nuclear matrix preparation, HeLa cells plated on cover slips were permeabilized with CSK buffer (100 mM NaCl, 300 mM sucrose, 10 mM pipes, pH 6.8, 3 mM $MgCl_2$, 1 mM EGTA, 1× solution of peptidase inhibitor cocktail, 0.5% Triton X-100) followed by DNase I (100 units/ml, Fermentas, Inc., USA) digestion at 37°C, extraction with 0.25 M ammonium sulfate (low salt) and 0.6 M ammonium sulfate (high salt). Multi-labeling of nuclear matrix associated proteins was performed on HeLa cells after appropriate extractions as described above.

THREE-DIMENSIONAL MICROSCOPY AND COMPUTER IMAGE ANALYSIS

Indirect immunofluorescence was detected with Chroma filter sets using an Olympus BX51 upright microscope (100 X plan-apo, oil, 1.4 NA) equipped with a Sensicam QE (Cooke Corporation, USA) digital charge-coupled device (CCD) camera, motorized *z*-axis controller (Prior) and Slidebook 4.0 software (Intelligent Imaging Innovations, Denver, CO). Optical sections were typically collected at 0.5 μm intervals through *z*-axis and processed using nearest-neighbor deconvolution (Slidebook 4.0) and exported as 16 bit tiff intensity files for further analysis.

SEGMENTATION AND PROXIMITY ANALYSIS OF FUNCTIONAL SITES

An improved knowledge based segmentation approach was developed based on earlier results from our group [Samarabandu et al., 1995; Ma et al., 1998]. The intensity surfaces of fluorescent spots follow an approximately exponential distribution and this property is used during the segmentation of the typical punctate structures observed in the nucleus. This spot-based method is currently the most suited algorithm for segmenting small-scale structures such as replication sites, transcription sites and other nuclear domains.

A "proximity" algorithm was developed that quantifies the spatial associations between different functional sites. After segmentation and centroid determination of sites, "Voronoi tessellation" [Preparata and Shamos, 1985] is performed for sites in one channel and the number of sites are counted in the comparison channel that are located in the computed cells at varying distances. Multi-labeling experiments are followed by segmentation of sites in all the individual channels. Pair-wise proximity relationships between different functions at various distances are plotted cumulatively. Fifteen or more representative mid-plane equivalent sections showing complete and uniform staining patterns for all the channels labeled are selected for analysis. Each mid plane equivalent section has hundreds of labeled sites all of which contribute to the total measurements. Standard error of the mean (SEM) values are indicated by *y*-axis error bars on the appropriate figures.

STATISTICAL ANALYSIS OF PROXIMITY RELATIONSHIPS

Cumulative distributions resulting from the proximity analysis between various functions (Fig. 3) were adjusted using the approximation of the cumulative normal function:

$$c = \frac{e^{2a_1(p-k)[1+a_2(p-k)^2]}}{1 + e^{2a_1(p-k)[1+a_2(p-k)^2]}}$$

where c is the cumulative number of nearest neighbors, p is the distance in pixels from the centroid, k determines the point of inflexion of the curve (i.e., the distance at which 50% of sites belonging to a certain function were found) and a_1 and a_2 determine the shape and intercept of the curve. Although random point distributions are typically described by the Poisson process, the normal distribution method used in our analysis provides satisfactory approximation when sample size is sufficiently large (>40) [Sokal and Rohlf, 1995]. Parameters a_1, a_2 and k were estimated by least-squares via the Quasi–Newton method. Regression residuals were used in unifactorial analysis of Variance (ANOVA) with 12 levels corresponding to the 12 proximity assignments. Tukey's HSD (honestly significant differences) test for unequal sample sizes was used for post hoc pair wise comparisons among levels. All analyses were conducted using STATISTICA 4.3 (Statsoft, 1993).

RESULTS

HIGH RESOLUTION IMAGING AND ANALYSIS OF FUNCTIONAL AND PROTEIN FACTOR SITE DISTRIBUTIONS IN THE CELL NUCLEUS

To characterize the distribution of functional and protein factor sites relative to each other in the cell nucleus, we performed simultaneous immunolabeling of HeLa cells for heterochromatin protein 1 gamma (HP1γ), nascent transcript sites (TS), RNA polymerase II sites (pol II), proliferating cell nuclear antigen (PCNA), and 4′,6-diamidino-2-phenylindole (DAPI is a stain which binds to the heterochromatin enriched areas more intensely). PCNA, a marker for active DNA replication sites [Leonhardt et al., 2000; Somanathan et al., 2001], enables identification of cells in early S-phase by a distinct nucleoplasmic punctate pattern [Nakayasu and Berezney, 1989; Vogel et al., 1989; Fox et al., 1991; Berezney, 2002; Dimitrova and Berezney, 2002]. Using indirect immunofluorescence, we found that the labeling for all the components examined is localized predominantly in punctate sites (refer to the red channel in Fig. 1A–D) of 0.2–0.4 μm diameter which are distributed throughout the extranucleolar interior. In addition, some larger sites of 0.4–0.7 μm were observed for HP1γ and pol II labeling. Line profile analysis was performed to evaluate the distribution of labeled sites with respect to the chromatin that was intensely stained by DAPI (Fig. 1A–D). HP1γ, a variant of heterochromatin protein 1, was predominantly localized to euchromatin (less intense DAPI stained regions) with occasional overlap (yellow arrows, Fig. 1C) of DAPI (green) and HP1γ (red) intensity peaks. The line profile analysis of TS, PCNA and pol II signals with respect to DAPI (Fig. 1B–D), also

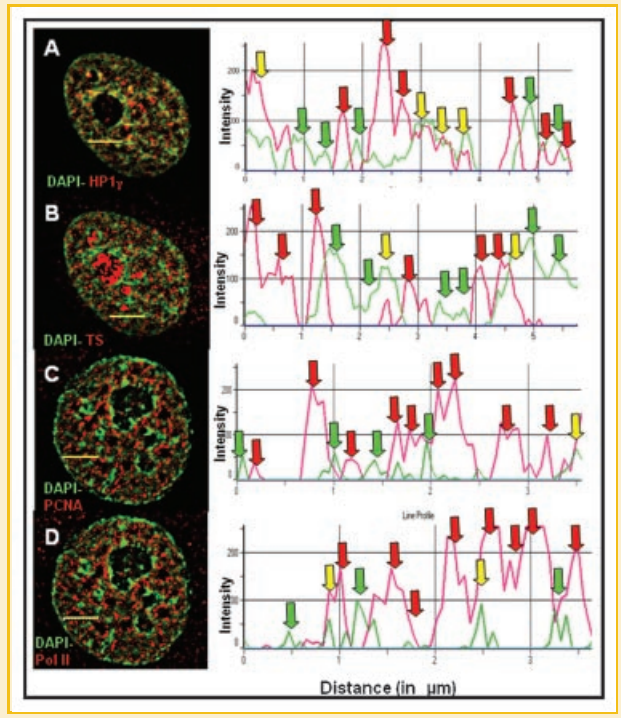

Fig. 1. Line profile analysis of functional sites in relation to heterochromatin. Representative mid plane sections of HeLa cell nuclei labeled for HP1γ–DAPI (A), TS–DAPI (B), PCNA–DAPI (C), and pol II–DAPI (D) were pseudocolored as indicated by the legend (DAPI in green, and functional/protein factor sites in red; primary antibodies against HP1γ and TS were labeled with anti-rabbit-IgG-Alexa594, anti-rat-IgG-Alexa647 respectively; and primary antibodies against PCNA and pol II were labeled with anti-rabbit-IgG-Alexa488 and anti-mouse-IgG-Alexa594 respectively in separate experiments). Images of individual channels were pseudocolored and overlaid for line profile analysis. Areas of the nucleus that are intensely stained with DAPI are considered to be enriched in heterochromatin. The green and the red peaks indicated in the line (yellow line across the image) profile correspond to the distribution of DAPI and functional sites respectively. The areas showing complete separation of red and green channel are indicated in the line profile by respective colored arrows. Regions of complete or large degree of overlap are indicated by yellow colored arrows.

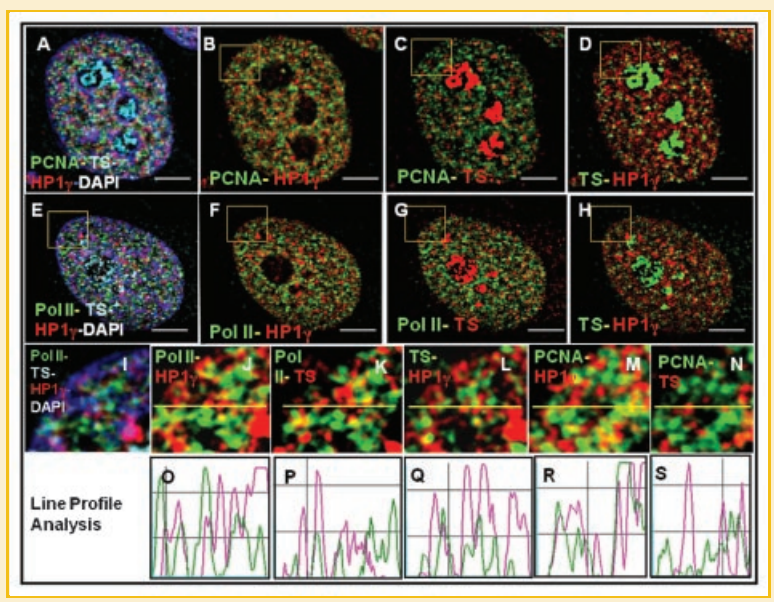

Fig. 2. Colocalization studies of multiple protein and functional sites in HeLa cells. A representative HeLa cell nucleus is shown multi-labeled for (A) PCNA, TS, HP1γ and DAPI. For (A) PCNA, TS, HP1γ and DAPI are pseudocolored in green (anti-mouse-IgG-Alexa488), cyan (anti-rat-IgG-Alexa647), red (anti-rabbit-IgG-Alexa594) and blue respectively. B–D show pair wise combination of different channels pseudocolored in red and green. Similarly, (E) shows a representative HeLa cell nucleus multi-labeled for pol II, TS, HP1γ and DAPI and subsequent pair wise combinations in green and red (F–H). Anti-mouse-IgG-Alexa488 is used as secondary antibody for pol II labeling. I–N represent magnified regions within the yellow boxes in panels (B–H). Line profile analysis of colocalization for the magnified regions (J–N) is shown in (O–S). White scale bars (A) to (H) indicate 5 μm.

indicated a predominant euchromatic distribution characterized by a marked separation from DAPI intense areas (separate red and green arrows on line profile, Figure 1B–D, occasional overlaps are depicted by yellow arrows).

PROXIMITY ANALYSIS OF FUNCTIONAL SITES

We next investigated the spatial distributions relative to each other of sites of pol II, early S-phase PCNA, HP1γ and TS. Individually labeled channels were pseudocolored in red-green combinations and overlaid in order to assess the extent of colocalization between sites (Fig. 2B–D,F–H,J–N). Multi-colored merged images exhibited complex patterns and varying degrees of overlaps among the different color channels (Fig. 2A,E,I). At higher magnification (Fig. 2J–N), significant levels of yellow colored sites (indicative of overlap) were detected among combinations of pol II-HP1γ, pol II-TS and PCNA-HP1γ sites. This finding was confirmed by line profile analysis (Fig. 2O–S), where colocalization between the channels is represented by the overlap of red and green peaks. Along with the overlapped peaks, separate red and green peaks are present (Fig. 2O–S) across the sampled yellow lines (Fig. 2J–N).

Correlation analysis among various fluorescently labeled biological structures is generally performed by methods such as Pearson's coefficient, Mander's coefficient, and "Caste" and Van Steensel's approach [Bolte and Cordelieres, 2006]. Analysis of the patterns observed in our studies by traditional colocalization methods, which are largely based on thresholding and pixel matching, do not adequately capture the complexity of the associations. To improve the analysis, we developed an object based computer image segmentation approach. The individual sites in each channel were segmented (see Materials and Methods Section), and the centroids were calculated. A newly developed proximity algorithm was then applied to determine the proximity relationship of one site to another measured as the pixel distance from centroid to centroid, independent of the intensity characteristics of sites (Fig. 3; also see Materials and Methods Section).

This proximity algorithm describes a unidirectional relationship between the compared sites. Under these conditions, the comparison of functions "A to B" may not be equal to that of "B to A." Twelve different combinations of proximity relationships (Fig. 3A) were determined among PCNA, pol II, HP1γ and TS. For example, "TS to Pol II" denotes the percentage of TS that are within a particular distance to the nearest pol II site. Similarly, 11 other proximity relationships were quantified (Fig. 3A) from the multi-labeling studies (Fig. 2). The x and y axes denote distance in pixels (1 pixel = 0.07 μm) and the percentage of sites within a particular distance to the sites of the channel being compared, respectively. Two categories of proximity relationships were determined as shown in Figure 3A. Pairs of sites whose centroid to centroid distances are less than 0.2 μm (1–3 pixels), indicate partial or complete overlap at the resolution of the light microscope. Centroid to centroid distances of the sites ranging between 0.2 and 0.5 μm (4–7 pixels), show various degrees of association from partial overlap to juxtaposition. The total proximity in the 1–7 pixel (0.5 μm) zone is then calculated as the sum of the 1–3 and 4–7 pixel values. The proximity data obtained in Figure 3A is further arranged as a matrix for proximity zones of 1–3 pixel and 1–7 pixels, respectively (Fig. 3B), For each zone, the first column of sites in each row denotes the reference sites under comparison. The second, third, and fourth columns of each row represent the neighboring functional sites in decreasing order of proximity.

A comprehensive statistical analysis indicated a high degree of significance for the differences in proximity distributions among the examined combinations. For example, the cumulative normal curve fits the proximity distributions remarkably well ($r^2 = 0.95$) and visual inspection of residual values graphed against distance in pixels revealed no higher order trend in the data. Estimated parameter values were $k = 4.47$, $a_1 = 0.34$ and $a_2 = -0.03$. ANOVA results employing residuals were highly significant ($F_{11,4998} = 95.42$, $P < 0.01$) and the residual distribution within each level did not depart significantly from normality.

Our results demonstrate that RNA polymerase II sites for both zones have the highest probability of being adjacent to a TS (TS-Pol II in Fig. 3A), whereas the other factors (HP1γ and PCNA) are in decreasing order of proximity (Fig. 3B). In terms of percentage of proximal TS within a 7 pixel distance, this corresponds to 91.1%, 81.8%, and 79.7%, for pol II, HP1γ and PCNA, respectively. The pol II sites also had the highest degree of proximity to the HP1γ (93.4%) and PCNA sites (92.0%). Identical patterns of proximity relationships were found for the 0.2 (1–3 pixel) and the 0.5 μm (1–7 pixel) zones. These distance relationships between functional sites are translated into a model, which is described in the Discussion Section (Fig. 7E). Notably, all of the percentage differences in proximity among pairs of sites in the comparison matrix (Fig. 3B) were determined to be statistically significant except between HP1γ to TS and HP1γ to PCNA. This indicates that HP1γ sites were equally proximal to TS and PCNA sites.

ANALYSIS OF NUCLEAR MATRIX PROTEINS AND THEIR RELATIONSHIP TO FUNCTIONAL AND PROTEIN FACTOR SITES

As a step toward characterizing the relationship of the early S PCNA, TS, and pol II sites to the nuclear matrix architecture, we included two abundant nuclear matrix proteins, matrin 3 and SAF-A in our analysis [Belgrader et al., 1991; Nakayasu and Berezney, 1991; Romig et al., 1992; Fackelmayer et al., 1994; Mattern et al., 1996]. Grey scale fluorescence intensities of labeled sites (Fig. 4A–D) were pseudocolored and overlaid for colocalization analysis (Fig. 4E,F). To reduce the complexity for image analysis, two channels were pseudocolored at a time in red and green as indicated in Figure 4G–L. Regions within these red-green pairs were enlarged (Fig. 4M–R) for line profile analysis (Fig. 4S–X). SAF-A, matrin 3 and pol II showed punctate patterns of sites with 0.2–0.4 μm diameter, which were distributed throughout the extranucleolar interior of the nucleus. Matrin 3 and SAF-A colocalize (yellow color) with certain intense DAPI areas indicating that they are not limited to euchromatic regions (Fig. 4M–N). This is consistent with earlier data on SAF-A localization in mouse heterochromatin [Lobov et al., 2001], and the role of SAF-A in X chromosome inactivation and XIST RNA immobilization [Helbig and Fackelmayer, 2003; Fackelmayer, 2005]. A significant level of overlap of matrin 3 and SAF-A is indicated by the yellow color (Fig. 4O) and by line profile analysis (Fig. 4U). Pol II and intense DAPI stained areas have little overlap, largely due to the preferential localization of pol II to euchromatic

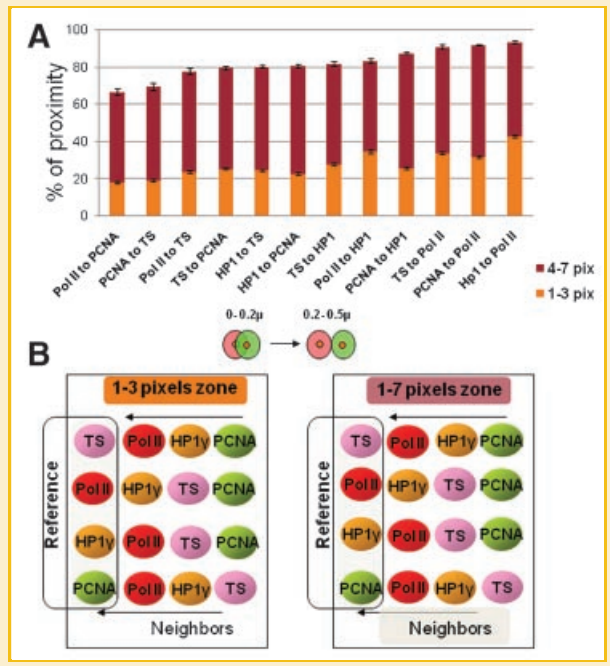

Fig. 3. Proximity analysis of multiple functional and protein factor sites. A: Plot shows the distribution of percentage proximity values of TS, pol II, HP1γ and PCNA to each other. Segmentation and centroid detection was followed by the proximity analysis for two components at a time. *x*-axis represents the distance in pixels (1 pixel = 0.07 μm) and *y*-axis represents the percent proximity. *y*-axis error bars denote the SEM. The proximity relationship between any two components was divided based on their centroid to centroid distance into two categories (1–3 pixels and 4–7 pixels). The red and green circles illustrate sites and indicate the two categories mentioned above which translate to approximate center-to-center distances of 0–0.2 μm and 0.2–0.5 μm. B,C: Proximity analysis matrix in which the centroid distances between the labeled sites were split into zones of "1–3" and "1–7" pixels, respectively. In each zone the first column represents the reference sites, while the second, third and fourth columns in each row show sites that are arranged in decreasing order of proximity to the reference.

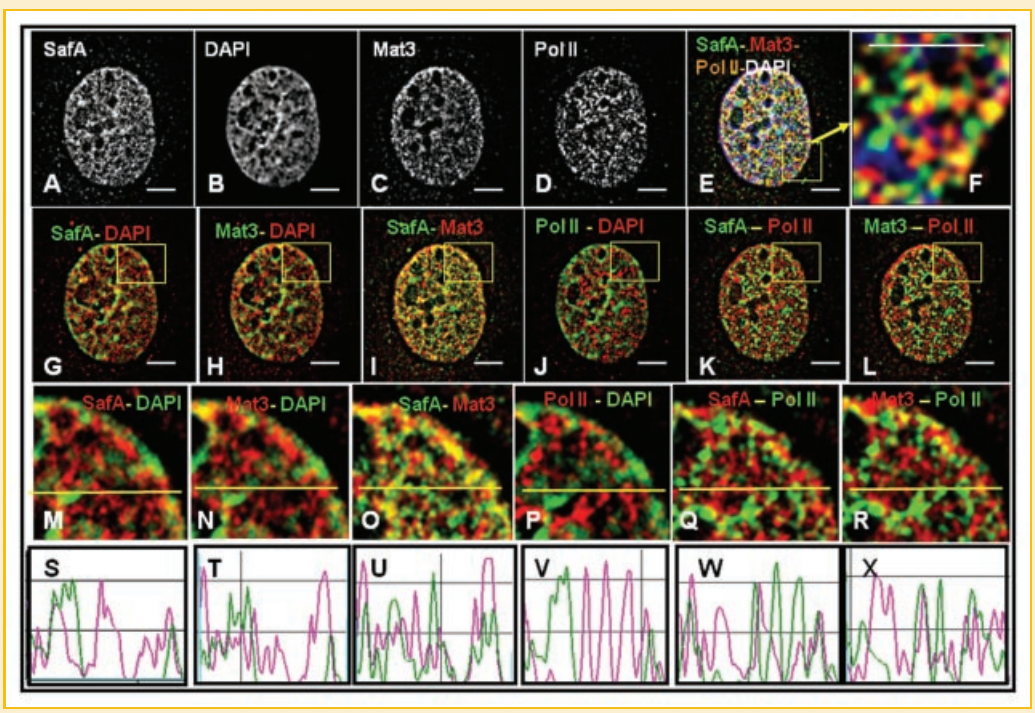

Fig. 4. Colocalization studies of multi-labeled HeLa cells for nuclear matrix proteins and RNA polymerase II. A–E: Grey scale intensities (better contrast) of a representative HeLa cell nucleus showing multi-labeling for SAF-A (A), DAPI (B), matrin 3 (C) and pol II (D) sites. (E) Merged and pseudocolored image of SAF-A (green, anti-rabbit-IgG-Alexa647), matrin 3 (red, anti-chicken-IgG-Alexa594), pol II (orange, anti-mouse-IgG-Alexa488) and DAPI (blue) signals. F: Enlarged image of the region represented by the yellow box in image (E). G–L: Pseudocolored pairwise overlays of the labeled channels in red and green as indicated by the color coded legend. Enlarged areas of (G–L) are shown in (M–R), respectively. Line profiles (S–X) represent the red and green channel intensities on the sampled yellow line in (M–R). White scale bars (A–L) represent 5 μm.

regions. Pol II sites exhibited varying degrees of overlaps with matrin 3 and SAF-A sites (Fig. 4Q,R,W,X). Multi-labeling experiments for matrin 3 and SAF-A sites with early S PCNA and TS sites (Fig. 5A–C) indicated a close association of the functional sites to the network-like distribution of matrin 3 and SAF-A.

The spatial associations of matrin 3 and SAF-A with pol II, TS and PCNA were then quantified using our proximity analysis program. Matrin 3 and SAF-A were highly proximal to each other (95% and 88.5% at 7 pixels for matrin 3 to SAF-A and SAF-A to matrin 3, respectively, Fig. 5D,E). They also demonstrated a high degree of association with PCNA (81.1% and 81.3%) and pol II sites (77% and 77.5%) for matrin 3 and SAF-A, respectively (Fig. 5D,E).

From these findings, it is enticing to consider that matrin 3 and SAF-A, along with other nuclear matrix proteins, establish a nuclear scaffolding network that forms a platform for supporting and regulating a variety of genomic functions in the chromatin and interchromatin compartments (Fig. 7D). Our high-resolution images of matrin 3 and SAF-A suggested that they form a network-like structure in the nucleus (Fig. 5A–C). To more precisely examine this possibility, we applied a MST algorithm to these images. This pattern recognition imaging approach connects the discrete sites identified following segmentation by a line path that follows aspects of nearest neighbor relationships between the centroids of the sites and a minimal distance for the entire pathway. Inspection at higher magnification demonstrate that the lines composing the MST network always pass through the raw signal in forming connections between the segmented sites and therefore accurately reflect the overall staining patterns of the images (Fig. 6A,B). The MST networks generated for matrin 3 (red) and SAF-A (green), while largely separate, are in strikingly close alignment and show many sites of colocalization (yellow color; Fig. 6E). Similar network-like patterns and colocalization for matrin 3 and SAF-A (Fig. 6H,I) and their corresponding MST structures (Fig. 6L) were observed following in situ extraction of cells for nuclear matrix. In contrast, the MST patterns formed by pol II sites in both cells before and after in situ extraction for nuclear matrix were spatially less closely aligned and showed no visible overlap with the network patterns of matrin 3 and SAF-A (Fig. 6 F,G,M,N).

DISCUSSION

ORGANIZATION OF FUNCTIONAL NEIGHBORHOODS IN THE NUCLEAR MICROENVIRONMENT

It is well known that diverse proteins form supra-molecular complexes and are organized in the form of punctate centers of activity inside the eukaryotic cell nucleus [Stein et al., 2007; Zaidi et al., 2007]. For example, both DNA replication and transcription occur within huge assemblies or ''factories'' within the nucleus each of which contains a multitude of replicons, genes and the associated protein factors involved in function and regulation [Jackson et al., 1993; Wansink et al., 1993; Hughes et al., 1995; Jackson, 2003]. Previous studies have demonstrated that the individual DNA replication and transcription factories are further arranged into higher order modules or *nuclear zones* [Wei et al., 1998]. It was proposed that these nuclear zones or *neighborhoods* provide the basis for the programming and coordination of replication and gene expression in the cell [Berezney and Wei, 1998; Berezney, 2002]. While the zones of replication and transcription in the cell nucleus are spatially separate, 3-D reconstruction studies suggested a very close proximity of these two different functional processes [Wei et al., 1998].

One implication of these findings is that protein factors that are involved in diverse genomic functions such as DNA replication and transcription may be concentrated together in these functional zones to enhance functional activity as well as to enable rapid switching between replicational and transcriptional processes as the cells traverse through their replicational and transcriptional programs [Berezney, 2002]. A recent microscopic analysis of ribosomal gene replication and transcription supports this view of a coordinate switching mechanism [Pliss et al., 2005]. Moreover, studies of several transcription factors and their spatial association to RNA polymerase II sites and sites of RNA synthesis demonstrated considerable differences in the degree of colocalization [Grande et al., 1997; Jackson et al., 2000; Choi et al., 2001; Elbi et al., 2002].

With this in mind, we have examined the spatial organization and proximity relationships of early S-phase replicating chromatin domains which are enriched in actively transcribed genes [MacAlpine et al., 2004; Schubeler et al., 2004], RNA polymerase II which mediates the transcription, nascent transcript sites (TS) which represent the product of transcription, and a chromatin associated protein, HP1γ, which has been implicated in transcriptional regulation. HP1 proteins are largely known for their association with transcriptional repression [Lehming et al., 1998]. The γ subtype of HP1, however, has been reported to associate with euchromatin and active genes [Minc et al., 2000; Lomberk et al., 2006; de Wit et al., 2007]. Although the role of a chromatin protein that is usually associated with repression of transcription is not clear in the context of euchromatin, it was speculated that it could mark the transcriptionally activated genes and prevent their reinitiation [Lomberk et al., 2006]. Recent identification of a specific phosphorylated form of HP1γ that colocalized with hyperphosphorylated RNA pol II, suggests these interactions of HP1γ as an additional layer of control for transcriptional regulation [Lomberk et al., 2006].

Cells processed for analysis were selected for early S-phase by their distinct replication pattern [Nakayasu and Berezney, 1989; Vogel et al., 1989; Fox et al., 1991; Dimitrova and Berezney, 2002] of PCNA (proliferating cell nuclear antigen), which is a general marker of active DNA replication. Central to the success of these experiments was the application of a spot-based segmentation program [Samarabandu et al., 1995; Ma et al., 1998] that enabled us to precisely position the centroid of each segmented site in a variety of multi-labeling protocols. To our knowledge, this program is without precedent in its ability to accurately distinguish sites that are in very close proximity and that vary widely in signal intensities [Ma et al., 1998; Wei et al., 1999]. With this as a basis, we developed a proximity program (see Materials and Methods Section) that measures the distance of one site to its nearest neighbor in another class of sites (e.g., the nearest TS to each HP1γ site). This enables us to go beyond the question of whether or not one site overlaps with another site in the nucleus and to address specific questions about the spatial relationships of multiple sites at the global level of the whole nucleus as well as within particular zones or functional

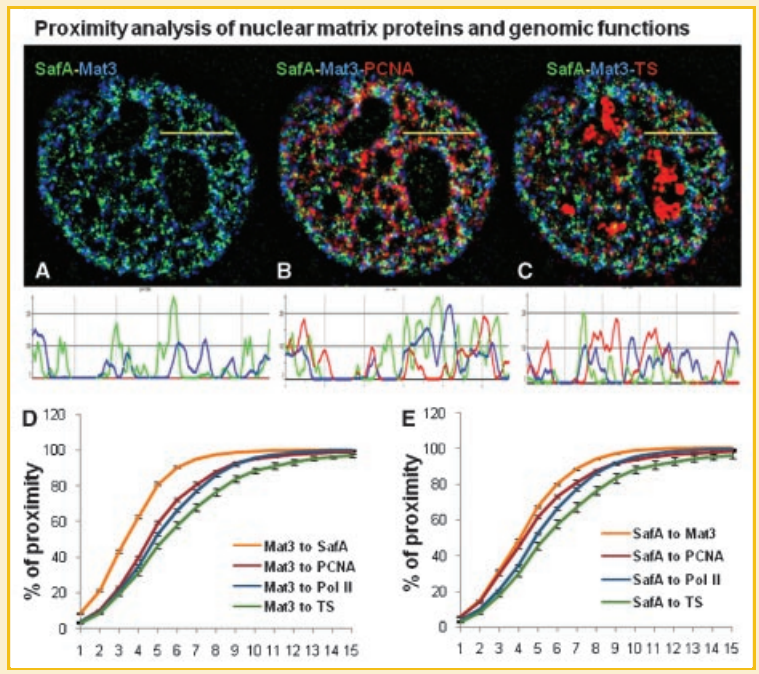

Fig. 5. Colocalization studies of nuclear matrix proteins, SAF-A and matrin 3 to PCNA, TS and pol II sites. Intact HeLa cell labeling of (A) SAF-A (green), matrin 3 (blue); (B) merged image of SAF-A (green), matrin 3 (blue) and PCNA (red) sites; (C) merged image of SAF-A (green), matrin 3 (blue) protein sites and TS (red). Intensely labeled nucleolar TS can be visualized in (C). Rabbit anti-SAF-A is detected with anti-rabbit-IgG-Alexa350; chicken anti-matrin 3 is detected with anti-chicken-Alexa594; mouse anti-GFP is detected with anti-mouse-IgG-Alexa488; and rat anti-BrdU is detected by anti-rat-IgG-Alexa647 antibodies. Line profiles of sampled yellow line for (A–C) are shown below the figures, respectively. Segmentation and centroid detection of nuclear images labeled for respective proteins and functions was followed by their pair wise proximity analysis. For the plots (D,E), *x*-axis represents the distance in pixels (1 pixel = 0.07 μm) and *y*-axis represents the percent (%) proximity. Standard error bars are indicated. The proximity relationship between labeled components (*y*-axis) is plotted as a cumulative function of distance (*x*-axis). D,E: Plots are shown depicting the results of proximity relationships between matrin 3 and SAF-A to TS, PCNA and pol II sites.

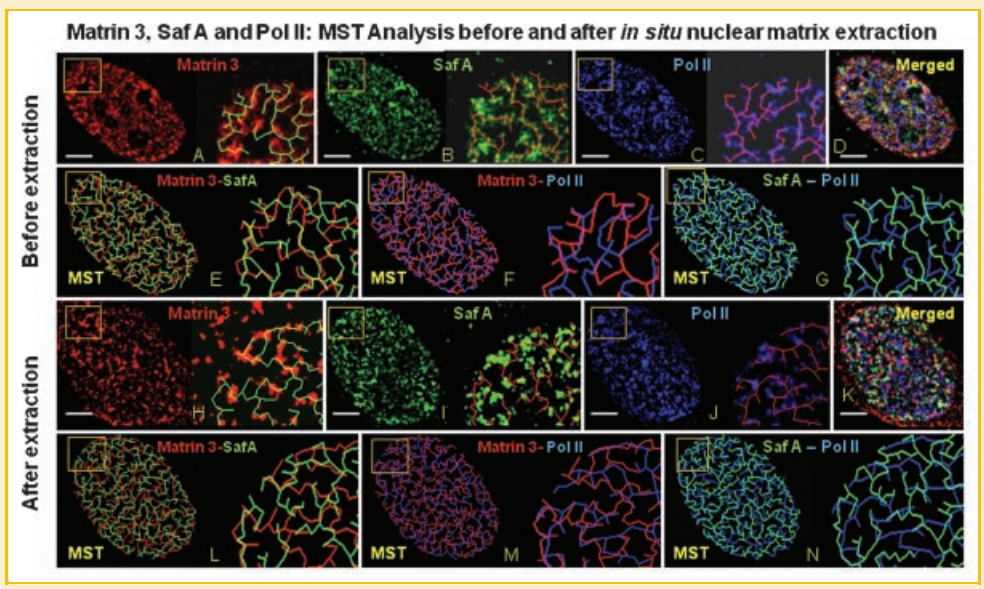

Fig. 6. MST analysis of matrin 3 and SAF-A sites before and after nuclear matrix extraction. A representative HeLa cell nucleus labeled in intact cells for nuclear matrix proteins matrin 3 (A, anti-chicken-IgG-Alexa594), SAF-A (B, anti-rabbit-IgG-Alexa488) and pol II (C, anti-mouse-IgG-Alexa647). Area within the yellow square is enlarged and overlaid with the minimal spanning tree (MST) which follows the raw fluorescent signal. Merged image of matrin 3 (red), SAF-A (green) and pol II (blue) staining (D). Overlays of minimal spanning trees of matrin 3 (red) and SAF-A (green) (E), matrin 3 (red) and pol II (blue) (F) and SAF-A (green) and pol II (blue) (G). Similarly, H–N indicates MST analysis after the extraction for nuclear matrix. Scale bars indicate 5 μm.

neighborhoods where sites of replication or transcription may be concentrated.

Our results demonstrate that PCNA (which defines early S-replicating chromatin domains that are enriched in actively transcribed genes), pol II, HP1γ and TS show strikingly high levels of proximity to each other wherein 75–95% of each site is within 7 pixels (0.5 μm) of a member of every other class of sites. This is consistent with the multi-labeling experiments for these sites (Fig. 2A,E,I) which show these multi-colored sites clustered in close apposition. We further found a spatial order to the proximity relationships between multiple functional sites (Fig. 3). For example, TS are closest to RNA pol II with over 90% within 7 pixels, followed by HP1γ and PCNA, at 81% and 79%, respectively. Pol II sites are also closest to HP1γ (83%) followed by PCNA (78%) and TS (67%). This suggests a degree of order to the spatial organization of these factors within the nuclear microenvironments.

The high levels of proximity of multiple functional sites and their enrichment in the transcriptionally active euchromatin, lead us to propose that the euchromatic regions of the nucleus are functionally organized into repeating zones or neighborhoods where there are close associations of both the functional sites of replication and transcription and the protein factors that mediate these processes into higher order combinatorial arrays (Fig. 7A–C). Based on the proximity relationships we can arrange the functional sites according to their probabilistic neighborhood distances as shown in Figure 7E. We further speculate on the function of this higher level organization for activation of gene transcription. As the DNA in an early S replicating chromatin domain (marked by PCNA) decondenses to engage in transcription, a proximal pol II site provides the enzymatic machinery to produce the nascent transcript (TS). Alternatively, chromatin could loop out to the periphery of the chromatin domain and engage with the transcription machinery in preassembled transcription factories [Hughes et al., 1995; Iborra et al., 1996; Osborne et al., 2004]. Similarly, HP1γ sites in the vicinity could provide the HP1γ protein to the elongating pol II complex for their deposition onto the newly transcribed regions of the gene [Minc et al., 2000; Lomberk et al., 2006].

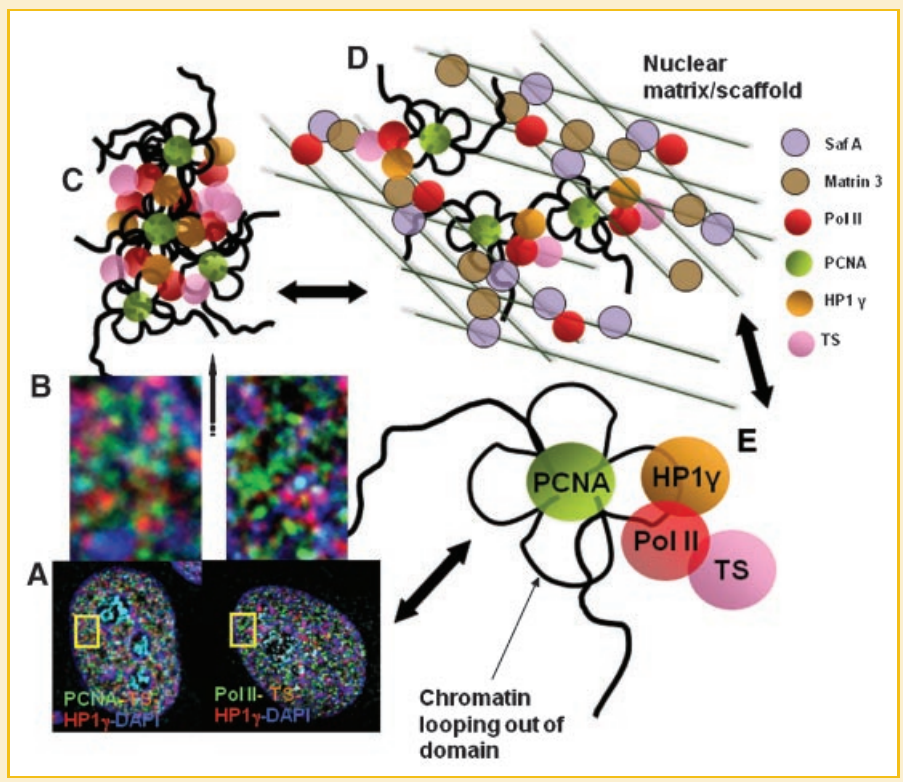

Fig. 7. A model for the organization of functional neighborhoods within the cell nucleus. Based on the results of microscopy of multi-labeling experiments (A,B), proximity relationships of protein and nuclear matrix factors to functional sites (Figs. 3 and 5), and pattern recognition analysis of matrin 3 and SAF-A using the MST algorithm for network organization (Fig. 6), a model is proposed for the organization of these functional neighborhoods (C) that are in close association with the nuclear matrix architecture (D). Due to their propensity to form network-like structures as revealed by MST analysis and a high degree of demonstrated spatial association (Fig. 5), the two abundant nuclear matrix proteins, namely, matrin 3 and SAF-A have been visualized as building blocks of the nuclear architecture (D). We emphasize, however, that many other protein factors are likely components of this overall nuclear matrix/scaffold network. Proximity analysis of these nuclear matrix proteins and labeled functional and protein factor sites predict a close association between a significant portion of them as illustrated in (D). These may represent matrin 3 and SAF-A sites that are actively involved in the function and/or regulation at closely associated functional sites. Other sites of matrin 3 and SAF-A that are more distal, contribute to the overall architecture of the nuclear matrix and may correspond to future sites for functional associations. Based on the proximity distances, the functional protein factor sites are hypothesized to be arranged in a specific order within the nuclear space (E). We propose that components of the nuclear matrix such as matrin 3 and SAF-A play a role in the dynamic formation of these functional arrays and serve as a platform for the assembly of multiple repeating patterns of sites that define a functional neighborhood in the cell nucleus (C,D).

RELATIONSHIP OF FUNCTIONAL NEIGHBORHOODS TO NUCLEAR ARCHITECTURE

The nuclear matrix has been proposed to be the *structural milieu* upon which nuclear functions and associated factors are organized in the cell nucleus [Berezney, 1984; Smith et al., 1984; Berezney et al., 1995, 1996; Wei et al., 1998; Berezney, 2002]. Indeed, many functionally related properties have been found associated with isolated nuclear matrix preparations and visualized after extraction of cells for nuclear matrix on cover slips [Berezney et al., 1995; Berezney, 2002]. In contrast, our understanding of the organization of specific proteins that compose the nuclear matrix architecture has lagged behind. With this in mind, we have examined the nuclear organization of two nuclear matrix associated proteins: matrin 3 [Belgrader et al., 1991] and SAF-A [Fackelmayer et al., 1994; Gohring and Fackelmayer, 1997; Martens et al., 2002] in relationship to the functional sites and factors investigated in this study.

SAF-A (120 kDa, 806 amino acids) is also known as hnRNP-U owing to its association with hnRNP particles and is a ubiquitous protein of the mammalian cell nucleus. Approximately half of the total SAF-A protein is present in the nuclear matrix. SAF-A binds to SAR/MAR DNA through an evolutionarily conserved SAF-box domain, which maps to the extreme amino terminus of the protein [Kipp et al., 2000]. Matrin 3 (125 kDa, 847 amino acids) was first isolated from rat liver nuclear matrix [Belgrader et al., 1991] where it is one of the major nuclear matrix proteins [Belgrader et al., 1991; Nakayasu and Berezney, 1991]. It is highly conserved in its amino acid sequence among mammals and contains characteristic N and C terminal zinc finger domains (referred to as ''matrin homology domains'') and two tandem RNA recognition motifs (RRM) [Belgrader et al., 1991; Hibino et al., 2006]. Its role in nuclear function has yet to be defined but it has been implicated in the processing of RNAs, mediating NMDA-induced neuronal death and also, possibly, in the modulation of MAR proximal promoter activity [Hibino et al., 2000; Zhang and Carmichael, 2001; Giordano et al., 2005]. Growth arrest by RNAi knockdown of matrin 3 in HeLa cells and gene disruption in chicken lymphoma (DT40) cells followed by rescue in both cases with full length chicken-matrin 3 further demonstrates an essential role of matrin 3 in cycling cells [Hisada-Ishii et al., 2007].

Multi-labeling of matrin 3, SAF-A, PCNA, pol II and TS in intact cells revealed that both matrin 3 and SAF-A were present in the same functional neighborhoods as the previously analyzed pol II, TS and PCNA. At higher magnifications, clustering of sites for each factor was observed with the different clusters of factors in close apposition (Fig. 4M–R). The discrete sites of matrin 3 and SAF-A showed significant levels of colocalization by direct visualization of yellow color and line profile analysis (Fig. 4O,U). Measurement of the proximities of matrin 3 and SAF-A (Fig. 5D,E) demonstrated a striking degree of proximity to each other (85–95% at 7 pixels) as well as with the functional sites (67–82% at 7 pixels). We, therefore, conclude that matrin 3 and SAF-A are components of the functional neighborhoods where genomic functions are concentrated. From a functional point of view, SAF-A has been implicated in the inhibition of the phosphorylation of CTD by TFIIH and subsequent repression of pol II elongation in vivo [Kim and Nikodem, 1999]. In contrast, the possible role of matrin 3 in transcriptional modulation has yet to be determined.

Previous studies of the nuclear matrix emphasized the network or framework structure after either extraction of isolated nuclei for nuclear matrix [Berezney and Coffey, 1974, 1977] or in situ preparation of cells grown on cover slips [Capco et al., 1982; Penman et al., 1982; Fey et al., 1986; Nickerson et al., 1997; Wan et al., 1999]. Demonstration of network structure for the nuclear matrix in intact cells has met with only limited success [Nalepa and Harper, 2004]. By applying a pattern recognition algorithm termed *MST*, we are able to visualize higher order network organization present within our images. Significantly, the lines that form the MST networks of matrin 3 and SAF-A accurately connect discretely labeled foci and follow closely the more diffusely stained labeling present between individual foci (Fig. 6A,B,H,I). Moreover, MST analysis of matrin 3 and SAF-A before and after extraction for nuclear matrix revealed a striking degree of close alignment and overlap associations between the two generated networks (Fig. 6E,L). In contrast, the MST higher order networks generated for pol II were spatially more distal from their matrin 3/SAF-A counterparts with no indication of direct overlap associations (Fig. 6F,G,M,N).

With this as a basis, we propose that matrin 3 and SAF-A are integral components of nuclear matrix architecture that serve as a platform for the dynamic assembly of functional zones of chromatin replication and transcription in the cell nucleus (Fig. 7D) and may potentially be directly involved in function (i.e., matrin 3 and SAF-A sites closest to the functional sites in Fig. 7D). Further studies combining high resolution 3-D microscopy with computer image analyses holds much promise for further elucidating the relationships of higher order chromatin organization, function and nuclear architecture.

ACKNOWLEDGMENTS

These studies were supported by NIH grant GM 072131 awarded to R.B. and NSF grant IIS-0713489 awarded to J.X.

REFERENCES

Albiez H, Cremer M, Tiberi C, Vecchio L, Schermelleh L, Dittrich S, Kupper K, Joffe B, Thormeyer T, von Hase J, Yang S, Rohr K, Leonhardt H, Solovei I, Cremer C, Fakan S, Cremer T. 2006. Chromatin domains and the interchromatin compartment form structurally defined and functionally interacting nuclear networks. Chromosome Res 14:707–733.

Belgrader P, Dey R, Berezney R. 1991. Molecular cloning of matrin 3. A. 125-kilodalton protein of the nuclear matrix contains an extensive acidic domain. J Biol Chem 266:9893–9899.

Berezney R. 1984. Organization and functions of nuclear matrix. In: Hnilica LS, editor. Chromosomal non-histone proteins. Boca Raton, FL: CRC Press. pp 119–180.

Berezney R. 2002. Regulating the mammalian genome: The role of nuclear architecture. Adv Enzyme Regul 42:39–52.

Berezney R, Coffey DS. 1974. Identification of a nuclear protein matrix. Biochem Biophys Res Commun 60:1410–1417.

Berezney R, Coffey DS. 1977. Nuclear matrix. Isolation and characterization of a framework structure from rat liver nuclei. J Cell Biol 73:616–637.

Berezney R, Wei X. 1998. The new paradigm: Integrating genomic function and nuclear architecture. J Cell Biochem Suppl 30–31:238–242.

Berezney R, Mortillaro MJ, Ma H, Wei X, Samarabandu J. 1995. The nuclear matrix: A structural milieu for genomic function. Int Rev Cytol 162A: 1–65.

Berezney R, Mortillaro M, Ma H, Meng C, Samarabandu J, Wei X, Somanathan S, Liou WS, Pan SJ, Cheng PC. 1996. Connecting nuclear architecture and genomic function. J Cell Biochem 62:223–226.

Bolte S, Cordelieres FP. 2006. A guided tour into subcellular colocalization analysis in light microscopy. J Microsc 224:213–232.

Capco DG, Wan KM, Penman S. 1982. The nuclear matrix: Three-dimensional architecture and protein composition. Cell 29:847–858.

Choi JY, Pratap J, Javed A, Zaidi SK, Xing L, Balint E, Dalamangas S, Boyce B, van Wijnen AJ, Lian JB, Stein JL, Jones SN, Stein GS. 2001. Subnuclear targeting of Runx/Cbfa/AML factors is essential for tissue-specific differentiation during embryonic development. Proc Natl Acad Sci USA 98:8650–8655.

Cook P. 1998. Duplicating a tangled genome. Science 281:1466–1467.

Cremer M, von Hase J, Volm T, Brero A, Kreth G, Walter J, Fischer C, Solovei I, Cremer C, Cremer T. 2001. Non-random radial higher-order chromatin arrangements in nuclei of diploid human cells. Chromosome Res 9:541–567.

Cremer T, Cremer M, Dietzel S, Muller S, Solovei I, Fakan S. 2006. Chromosome territories–a functional nuclear landscape. Curr Opin Cell Biol 18:307–316.

de Wit E, Greil F, van Steensel B. 2007. High-resolution mapping reveals links of HP1 with active and inactive chromatin components. PLoS Genet 3:e38.

Dimitrova DS, Berezney R. 2002. The spatio-temporal organization of DNA replication sites is identical in primary, immortalized and transformed mammalian cells. J Cell Sci 115:4037–4051.

Dundr M, Misteli T. 2001. Functional architecture in the cell nucleus. Biochem J 356:297–310.

Dussert C, Rasigni M, Palmari J, Rasigni G, Llebaria A, Marty F. 1987. Minimal spanning tree analysis of biological structures. J Theor Biol 125:317–323.

Dussert C, Rasigni G, Llebaria A. 1988. Quantization of directional properties in biological structures using the minimal spanning tree. J Theor Biol 135: 295–302.

Elbi C, Misteli T, Hager GL. 2002. Recruitment of dioxin receptor to active transcription sites. Mol Biol Cell 13:2001–2015.

Fackelmayer FO. 2005. A stable proteinaceous structure in the territory of inactive X chromosomes. J Biol Chem 280:1720–1723.

Fackelmayer FO, Dahm K, Renz A, Ramsperger U, Richter A. 1994. Nucleic-acid-binding properties of hnRNP-U/SAF-A, a nuclear-matrix protein which binds DNA and RNA in vivo and in vitro. Eur J Biochem 221:749–757.

Fey EG, Ornelles DA, Penman S. 1986. Association of RNA with the cytoskeleton and the nuclear matrix. J Cell Sci (Suppl 5):99–119.

Fox MH, Arndt-Jovin DJ, Jovin TM, Baumann PH, Robert-Nicoud M. 1991. Spatial and temporal distribution of DNA replication sites localized by immunofluorescence and confocal microscopy in mouse fibroblasts. J Cell Sci 99:247–253.

Giordano G, Sanchez-Perez AM, Montoliu C, Berezney R, Malyavantham K, Costa LG, Calvete JJ, Felipo V. 2005. Activation of NMDA receptors induces protein kinase A-mediated phosphorylation and degradation of matrin 3. Blocking these effects prevents NMDA-induced neuronal death. J Neurochem 94:808–818.

Gohring F, Fackelmayer FO. 1997. The scaffold/matrix attachment region binding protein hnRNP-U (SAF-A) is directly bound to chromosomal DNA in vivo: A chemical cross-linking study. Biochemistry 36:8276–8283.

Grande MA, van der Kraan I, de Jong L, van Driel R. 1997. Nuclear distribution of transcription factors in relation to sites of transcription and RNA polymerase II. J Cell Sci 110(Pt 15): 1781–1791.

Helbig R, Fackelmayer FO. 2003. Scaffold attachment factor A (SAF-A) is concentrated in inactive X chromosome territories through its RGG domain. Chromosoma 112:173–182.

Hendzel MJ, Kruhlak MJ, MacLean NA, Boisvert F, Lever MA, Bazett-Jones DP. 2001. Compartmentalization of regulatory proteins in the cell nucleus. J Steroid Biochem Mol Biol 76:9–21.

Hibino Y, Ohzeki H, Sugano N, Hiraga K. 2000. Transcription modulation by a rat nuclear scaffold protein, P130, and a rat highly repetitive DNA component or various types of animal and plant matrix or scaffold attachment regions. Biochem Biophys Res Commun 279:282–287.

Hibino Y, Usui T, Morita Y, Hirose N, Okazaki M, Sugano N, Hiraga K. 2006. Molecular properties and intracellular localization of rat liver nuclear scaffold protein P130. Biochim Biophys Acta 1759:195–207.

Hisada-Ishii S, Ebihara M, Kobayashi N, Kitagawa Y. 2007. Bipartite nuclear localization signal of matrin 3 is essential for vertebrate cells. Biochem Biophys Res Commun 354:72–76.

Hughes TA, Pombo A, McManus J, Hozak P, Jackson DA, Cook PR. 1995. On the structure of replication and transcription factories. J Cell Sci Suppl 19:59–65.

Iborra FJ, Pombo A, Jackson DA, Cook PR. 1996. Active RNA polymerases are localized within discrete transcription ''factories'' in human nuclei. J Cell Sci 109(Pt 6): 1427–1436.

Jackson DA. 2003. The anatomy of transcription sites. Curr Opin Cell Biol 15:311–317.

Jackson DA, Pombo A. 1998. Replicon clusters are stable units of chromosome structure: Evidence that nuclear organization contributes to the efficient activation and propagation of S phase in human cells. J Cell Biol 140:1285–1295.

Jackson DA, Hassan AB, Errington RJ, Cook PR. 1993. Visualization of focal sites of transcription within human nuclei. EMBO J 12:1059–1065.

Jackson DA, Pombo A, Iborra F. 2000. The balance sheet for transcription: An analysis of nuclear RNA metabolism in mammalian cells. FASEB J 14:242–254.

Kim MK, Nikodem VM. 1999. hnRNP U inhibits carboxy-terminal domain phosphorylation by TFIIH and represses RNA polymerase II elongation. Mol Cell Biol 19:6833–6844.

Kipp M, Gohring F, Ostendorp T, van Drunen CM, van Driel R, Przybylski M, Fackelmayer FO. 2000. SAF-Box, a conserved protein domain that specifically recognizes scaffold attachment region DNA. Mol Cell Biol 20:7480–7489.

Lehming N, Le Saux A, Schuller J, Ptashne M. 1998. Chromatin components as part of a putative transcriptional repressing complex. Proc Natl Acad Sci USA 95:7322–7326.

Leonhardt H, Rahn HP, Weinzierl P, Sporbert A, Cremer T, Zink D, Cardoso MC. 2000. Dynamics of DNA replication factories in living cells. J Cell Biol 149:271–280.

Lobov IB, Tsutsui K, Mitchell AR, Podgornaya OI. 2001. Specificity of SAF-A and lamin B binding in vitro correlates with the satellite DNA bending state. J Cell Biochem 83:218–229.

Lomberk G, Bensi D, Fernandez-Zapico ME, Urrutia R. 2006. Evidence for the existence of an HP1-mediated subcode within the histone code. Nat Cell Biol 8:407–415.

Ma H, Samarabandu J, Devdhar RS, Acharya R, Cheng PC, Meng C, Berezney R. 1998. Spatial and temporal dynamics of DNA replication sites in mammalian cells. J Cell Biol 143:1415–1425.

MacAlpine DM, Rodriguez HK, Bell SP. 2004. Coordination of replication and transcription along a Drosophila chromosome. Genes Dev 18:3094–3105.

Martens JH, Verlaan M, Kalkhoven E, Dorsman JC, Zantema A. 2002. Scaffold/matrix attachment region elements interact with a p300-scaffold attachment factor A complex and are bound by acetylated nucleosomes. Mol Cell Biol 22:2598–2606.

Mattern KA, Humbel BM, Muijsers AO, de Jong L, van Driel R. 1996. hnRNP proteins and B23 are the major proteins of the internal nuclear matrix of HeLa S3 cells. J Cell Biochem 62:275–289.

McManus KJ, Stephens DA, Adams NM, Islam SA, Freemont PS, Hendzel MJ. 2006. The transcriptional regulator CBP has defined spatial associations within interphase nuclei. PLoS Comput Biol 2:e139.

Meaburn KJ, Misteli T. 2007. Cell biology: Chromosome territories. Nature 445:379–781.

Minc E, Courvalin JC, Buendia B. 2000. HP1gamma associates with euchromatin and heterochromatin in mammalian nuclei and chromosomes. Cytogenet Cell Genet 90:279–284.

Misteli T. 2007. Beyond the sequence: Cellular organization of genome function. Cell 128:787–800.

Mitchell JA, Fraser P. 2008. Transcription factories are nuclear subcompartments that remain in the absence of transcription. Genes Dev 22:20–25.

Nakayasu H, Berezney R. 1989. Mapping replicational sites in the eucaryotic cell nucleus. J Cell Biol 108:1–11.

Nakayasu H, Berezney R. 1991. Nuclear matrins: Identification of the major nuclear matrix proteins. Proc Natl Acad Sci USA 88:10312–10316.

Nalepa G, Harper JW. 2004. Visualization of a highly organized intranuclear network of filaments in living mammalian cells. Cell Motil Cytoskeleton 59:94–108.

Nickerson JA, Krockmalnic G, Wan KM, Penman S. 1997. The nuclear matrix revealed by eluting chromatin from a cross-linked nucleus. Proc Natl Acad Sci USA 94:4446–4450.

Osborne CS, Chakalova L, Brown KE, Carter D, Horton A, Debrand E, Goyenechea B, Mitchell JA, Lopes S, Reik W, Fraser P. 2004. Active genes dynamically colocalize to shared sites of ongoing transcription. Nat Genet 36:1065–1071.

Penman S, Fulton A, Capco D, Ben Ze'ev A, Wittelsberger S, Tse CF. 1982. Cytoplasmic and nuclear architecture in cells and tissue: Form, functions, and mode of assembly. Cold Spring Harb Symp Quant Biol 46(Pt 2):1013–1028.

Pliss A, Koberna K, Vecerova J, Malinsky J, Masata M, Fialova M, Raska I, Berezney R. 2005. Spatio-temporal dynamics at rDNA foci: Global switching between DNA replication and transcription. J Cell Biochem 94:554–565.

Preparata FP, Shamos MI. 1985. An introduction. Computational geometry. New York: Springer-Verlag. p 398.

Razin SV, Iarovaia OV, Sjakste N, Sjakste T, Bagdoniene L, Rynditch AV, Eivazova ER, Lipinski M, Vassetzky YS. 2007. Chromatin domains and regulation of transcription. J Mol Biol 369:597–607.

Romig H, Fackelmayer FO, Renz A, Ramsperger U, Richter A. 1992. Characterization of SAF-A, a novel nuclear DNA binding protein from HeLa cells with high affinity for nuclear matrix/scaffold attachment DNA elements. EMBO J 11:3431–3440.

Sadoni N, Cardoso MC, Stelzer EH, Leonhardt H, Zink D. 2004. Stable chromosomal units determine the spatial and temporal organization of DNA replication. J Cell Sci 117:5353–5365.

Samarabandu J, Ma H, Acharya R, Cheng PC, Berezney R. 1995. Image analysis techniques for visualizing the spatial organization of DNA replication sites in the mammalian cell nucleus using multi-channel confocal microscopy. SPIE 2434:370–375.

Schubeler D, MacAlpine DM, Scalzo D, Wirbelauer C, Kooperberg C, van Leeuwen F, Gottschling DE, O'Neill LP, Turner BM, Delrow J, Bell SP, Groudine M. 2004. The histone modification pattern of active genes revealed through genome-wide chromatin analysis of a higher eukaryote. Genes Dev 18:1263–1271.

Skalnikova M, Bartova E, Ulman V, Matula P, Svoboda D, Harnicarova A, Kozubek M, Kozubek S. 2007. Distinct patterns of histone methylation and acetylation in human interphase nuclei. Physiol Res 56:797–806.

Smith HC, Puvion E, Buchholtz LA, Berezney R. 1984. Spatial distribution of DNA loop attachment and replicational sites in the nuclear matrix. J Cell Biol 99:1794–1802.

Sokal RR, Rohlf FJ. 1995. Biometry. San Francisco: WH Freeman and Company.

Somanathan S, Suchyna TM, Siegel AJ, Berezney R. 2001. Targeting of PCNA to sites of DNA replication in the mammalian cell nucleus. J Cell Biochem 81:56–67.

Stein GS, van Wijnen AJ, Stein JL, Lian JB. 1999. Interrelationships of transcriptional machinery with nuclear architecture. Crit Rev Eukaryot Gene Expr 9:183–190.

Stein GS, Lian JB, Stein JL, van Wijnen AJ, Montecino M, Pratap J, Choi J, Zaidi SK, Javed A, Gutierrez S, Harrington K, Shen J, Young D. 2003a. Intranuclear organization of RUNX transcriptional regulatory machinery in biological control of skeletogenesis and cancer. Blood Cells Mol Dis 30:170–176.

Stein GS, Zaidi SK, Braastad CD, Montecino M, van Wijnen AJ, Choi JY, Stein JL, Lian JB, Javed A. 2003b. Functional architecture of the nucleus: Organizing the regulatory machinery for gene expression, replication and repair. Trends Cell Biol 13:584–592.

Stein GS, Lian JB, van Wijnen AJ, Stein JL, Javed A, Montecino M, Zaidi SK, Young D, Choi JY, Gutierrez S, Pockwinse S. 2004. Nuclear microenvironments support assembly and organization of the transcriptional regulatory machinery for cell proliferation and differentiation. J Cell Biochem 91:287–302.

Stein GS, Lian JB, Stein JL, van Wijnen AJ, Javed A, Montecino M, Zaidi SK, Young DW, Choi JY, Pratap J. 2005. Combinatorial organization of the transcriptional regulatory machinery in biological control and cancer. Adv Enzyme Regul 45:136–154.

Stein GS, Lian JB, van Wijnen AJ, Stein JL, Javed A, Montecino M, Choi JY, Vradii D, Zaidi SK, Pratap J, Young D. 2007. Organization of transcriptional regulatory machinery in nuclear microenvironments: Implications for biological control and cancer. Adv Enzyme Regul 47:242–250.

Strouboulis J, Wolffe AP. 1996. Functional compartmentalization of the nucleus. J Cell Sci 109(Pt 8): 1991–2000.

Verschure PJ, Van Der Kraan I, Enserink JM, Mone MJ, Manders EM, Van Driel R. 2002. Large-scale chromatin organization and the localization of proteins involved in gene expression in human cells. J Histochem Cytochem 50:1303–1312.

Vogel W, Autenrieth M, Mehnert K. 1989. Analysis of chromosome replication by a BrdU antibody technique. Chromosoma 98:335–341.

Wan KM, Nickerson JA, Krockmalnic G, Penman S. 1999. The nuclear matrix prepared by amine modification. Proc Natl Acad Sci USA 96:933–938.

Wansink DG, Schul W, van der Kraan I, van Steensel B, van Driel R, de Jong L. 1993. Fluorescent labeling of nascent RNA reveals transcription by RNA polymerase II in domains scattered throughout the nucleus. J Cell Biol 122:283–293.

Wei X, Samarabandu J, Devdhar RS, Siegel AJ, Acharya R, Berezney R. 1998. Segregation of transcription and replication sites into higher order domains. Science 281:1502–1506.

Wei X, Somanathan S, Samarabandu J, Berezney R. 1999. Three-dimensional visualization of transcription sites and their association with splicing factor-rich nuclear speckles. J Cell Biol 146:543–558.

Young DW, Zaidi SK, Furcinitti PS, Javed A, van Wijnen AJ, Stein JL, Lian JB, Stein GS. 2004. Quantitative signature for architectural organization of regulatory factors using intranuclear informatics. J Cell Sci 117:4889–4896.

Zaidi SK, Javed A, Pratap J, Schroeder TM, JW J, Lian JB, van Wijnen AJ, Stein GS, Stein JL. 2006. Alterations in intranuclear localization of Runx2 affect biological activity. J Cell Physiol 209:935–942.

Zaidi SK, Young DW, Javed A, Pratap J, Montecino M, van Wijnen A, Lian JB, Stein JL, Stein GS. 2007. Nuclear microenvironments in biological control and cancer. Nat Rev Cancer 7:454–463.

Zhang Z, Carmichael GG. 2001. The fate of dsRNA in the nucleus: A p54(nrb)-containing complex mediates the nuclear retention of promiscuously A-to-I edited RNAs. Cell 106:465–475.

Zinner R, Albiez H, Walter J, Peters AH, Cremer T, Cremer M. 2006. Histone lysine methylation patterns in human cell types are arranged in distinct three-dimensional nuclear zones. Histochem Cell Biol 125:3–19.